Formation and Optical Properties of Compression-Induced Nanoscale Buckles on Silver Nanowires

Nathan L. Netzer,[†] Ray Gunawidjaja,[‡] Marie Hiemstra,[†,§] Qiang Zhang,[†] Vladimir V. Tsukruk,[‡] and Chaoyang Jiang[†,*]

[†]Department of Chemistry, University of South Dakota, Vermillion, South Dakota 57069, and [‡]School of Materials Science and Engineering, Georgia Institute of Technology, Atlanta, Georgia 30332. [§]Current address: Azusa Pacific University.

ABSTRACT An intriguing formation of nanoscale buckles is discovered when an array of aligned silver nanowires was deposited onto prestrained polydimethylsiloxane substrates. The spacing distance between the resulting silver nanoparticles corresponds to the buckling wavelength of the silver nanowires. The buckled nanowires exhibit unique optical properties, such as interruption of scattered polarized photons and emission of photons from subwavelength structure, as well as surface-enhanced Raman scattering at the vicinity of the formed nanobuckles. In this way, they have great potentials for nano-opto devices, catalysts for chemical reactions, and functional materials for chemical detections.

One-dimensional metallic nanomaterials with tunable size and shape attract increasing interests in both fundamental studies and practical applications due to their unique electrical, optical, mechanical, and chemical properties.[1−5] A variety of methods has been developed for preparing silver nanorods (NRs) and silver nanowires (NWs), such as deposition in nanoporous alumina membranes,[6] wet chemical synthesis with surfactant,[7] microwave-assisted assembly,[8−10] and template-based synthesis from DNA[11] or carbon nanotubes.[12] The application of one-dimensional silver NRs and NWs can range from catalytic property,[13] photonic materials, and plasmonic waveguide,[14] to active substrates for surface-enhanced Raman scattering (SERS).[15] Constructing nanoparticle/nanowire hybrids and manipulating their optical properties are intriguing for their localized surface plasmon resonance (LSPR).[16−20] For example, Uji-I and co-workers decorated silver NWs with dense silver nanoparticles (NPs) by self-assembly process and observed well-separated and fairly regular hot-spots of LSPRs.[19] Mirkin and co-workers synthesized a gold nanodisk array by using on-wire lithography, where the precisely controlled disk thickness and interparticle gap are critical in forming SERS hot-spots.[21,22] However, a fundamental challenge remains in the facile fabrication of hybrid silver nanostructures with predetermined and spatially controlled LSPR hot-spots. Such nanoscale hybrids will have great potentials in ultrahigh sensitive chemical and biological detections.

Meanwhile, mechanical behavior of nanomaterials have attracted more attentions because of their importance in developing new generations of nanowire-based

devices.[23−28] Size dependence of nanomechanical behaviors of silver NWs has been observed and discussed.[29,30] Aston *et al.* studied nanomechanical bending behavior and elastic modulus of silver NWs by using digital pulsed force mode atomic force microscopy (AFM) and calculated the elastic modulus for as-prepared silver NWs based on classical modeling.[31] An anisotropic mechanical response of nanocomposite multilayer films encapsulated silver NWs were reported recently.[32] The buckling phenomena of silver nanowires were utilized to evaluate the Young's modulus of silver NWs. Such matrix-induced buckling phenomena can be applied as a fast approach in measuring the elastic modulus of nanowires with a good precision. To the best of our knowledge, there are limited accounts on the study of plastic deformation of one-dimensional silver nanowires.

Here we report intriguing and unexpected results on detailed characterizations on formations, structures, and optical properties of nanoscale buckles that were formed on compressed silver nanowires. By applying compressive-stress to highly oriented silver nanowires that are immobilized
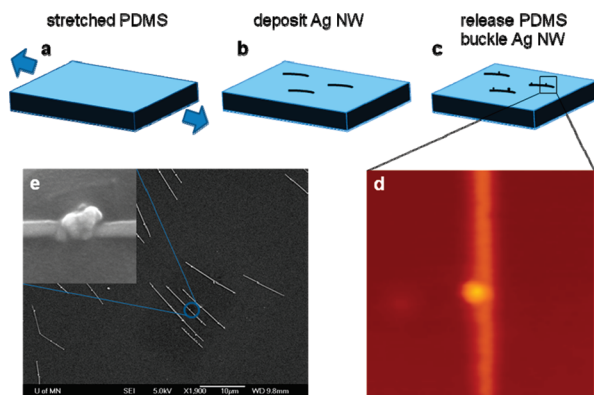
Figure 1. Schematics and images of silver nanobuckles: (a−c) compression-induced silver nanobuckles formation by depositing silver nanowires onto a prestrained PDMS substrate; (d) AFM image of silver nanobuckle formed on a silver nanowire (image size: 5 × 5 μm²); (e) SEM micrograph of silver nanobuckles along the silver nanowires. (Inset) A higher magnification (25000×), side-view (tilt angle, 30°) SEM micrograph of a silver nanobuckle.

on a polydimethylsiloxane (PDMS) substrate, we observed the formation of nanobuckles on initially "smooth" silver nanowires. The nanoscale buckles were stable in ambient conditions and their morphologies and structures were characterized with AFM and scanning electron microscopy (SEM). We have used the term nanobuckle because the spacing distance between these structures corresponds to its buckling wavelength. A mechanism based on the buckling theory of a one-dimensional rod is proposed in this manuscript to explain the formation of these nanobuckles on silver NWs. Such nanobuckles can have significant impact on the 1D propagation of surface plasmon, a collective electron resonance in silver NWs. Furthermore, we studied scattering photons from these nanobuckles by guiding a laser beam onto neighboring nanobuckle or wire end. Confocal SERS measurements of the buckled silver nanowires were conducted and the results revealed that enhancement of Raman signals can be modulated by the presence of silver nanobuckles.

RESULTS AND DISCUSSION

Our method provides a simple, unique, and novel approach in synthesizing nanobuckles on silver nanowires. As shown in Figure 1, silver nanowires were initially deposited from methanol suspension onto a mechanically prestrained (*i.e.,* over 10% strain) PDMS substrate. Upon releasing the prestrain, the PDMS substrate returns to its original shape, during which nanoscale buckles were unexpectedly formed owing to the shear stress on the silver nanowires because of the strong adhesion between silver NWs and PDMS substrate (Figure 1b,c). Such phenomenon is quite similar to the molecular buckling of individual single-walled carbon nanotubes (CNTs) on elastomeric substrate that was reported recently.[33] While in their study, the authors obtained a wavy morphology of the buckled carbon nano-

tubes due to buckling instability, we only observed some nanoscale particles, named here as nanobuckles, appearing along the silver nanowires, and there are no wavy features observed for the silver nanowires. Figure 1d shows a typical AFM image of a nanobuckle that is formed along a silver nanowire. The different mechanical response for CNTs and silver nanowires may be associated with the differences in their elastic modulus and structures, including the shapes and diameters.

Although a full understanding on the mechanism on the formation of nanoscale buckles is still in progress, the nanobuckles usually formed within three days after the prestrained PDMS onto which silver NWs reside was released and can be observed on most of the silver NWs. Figure 1e shows a typical SEM micrograph of these nanobuckles, from which we can clearly find that most silver NWs can have more than one nanobuckle. The inset one in Figure 1e presented a higher resolution side view SEM image of a nanoscale buckle by tilting the SEM sample at an angle of 30°. It is clearly demonstrated that the silver nanobuckle has a size below 100 nm and an irregular shape, which is quite different as compared to silver nanoparticles grown from normal wet chemistry methods.[19] Further understanding of the irregular silver nanoparticles might result to some unique applications, such as catalysis for chemical reactions.

Optical micrographs of the silver NWs with nanobuckles were recorded by a three-megapixel CCD camera that is attached to an Aramis confocal microscope. A white light beam from an EFP-5H lamp was used to illuminate the sample and normal bright field mode was applied in obtaining the optical micrographs. These optical micrographs were used as a guide map for the AFM imaging. As shown in Figure 2a, the silver nanowires give higher intensity with respect to the underlying substrate (PDMS) owing to their high reflectivity and strong photon scattering. It is interesting that the nanobuckles along the silver NWs appeared "dark" in the optical image, which provides a clear sense regarding the location and distribution of the silver nanobuckles. The detail study on the optical properties of nanobuckles will be discussed below. Nevertheless, a large-area view of the sample with optical microscopy can make it more efficient in further AFM studies by providing micrometer scale mapping on the nanobuckles on silver nanowire.

There is a certain correlation between the spacing of the nanobuckles on the silver nanowire and the diameter of the silver NW, as revealed by the AFM investigations. Figure 2b shows a representative AFM image of silver nanobuckles. Similar to the results of SEM observation, nanobuckles were formed along the silver nanowires and, quite often, there are several nanobuckles on one individual nanowire. Furthermore, we found that the distances between the nanobuckles on the same silver NW are quite close, which can be explained

with a Newtonian analytical mechanics model that uses linear elasticity theory.[34] We approximate the silver NW as a solid rod with a radius R and Young's modulus E_{Ag}. The PDMS substrate is modeled as a semi-infinite solid with Young's modulus E_S and Poisson's ratio ν_S. The plane-strain modulus of PDMS is noted as $\bar{E}_S = E_S/(1 - \nu_S^2)$. According to the buckling theory,[33] k, wavevector, where $k = 2\pi/\lambda$, λ is the distance between the nanobuckles, can be approximated as

$$k = \frac{3}{4}\left(\frac{\overline{E}_S}{E_{Ag}I}\right)^{1/4} \tag{1}$$

where $I = \pi R^4/4$ is the moment of inertia of the silver nanowires. According to eq 1, a linear relationship between the nanobuckle distance and the radius of the silver nanowires is expected. By using AFM, we have measured the distances between the nanobuckles along the individual silver nanowire and the diameters of silver nanowires at 45 different locations. The results shown in Figure 2d clearly demonstrate the trend that a larger distance of nanobuckles appears from thicker silver nanowires. With the average radius being 39.0 ± 6.8 nm and average distance being 4.3 ± 1.1 μm between neighboring nanobuckles, the elastic moduli of silver nanowires were calculated to be about 91.3 GPa. A solid line was also drawn on Figure 2d based on the calculation with eq 1. The Young's modulus measured with the current method is similar to those measured for silver NWs by nanoindentation (83−93 GPa)[29] and AFM bending tests (80−96.4 GPa),[31] while being a little bit lower than those determined by nanowire buckling of direct force displacement measurements (100−120 GPa)[35] and matrix-assisted buckling of silver NW/polymer composites (118 GPa).[32]

By closely investigating with higher magnification AFM, we found that the size of silver nanobuckles was quite inconsistent on some of the silver NWs. As shown in Figure 2c, a small silver nanobuckle (indicated by the arrow) appears in the middle of normal size nanobuckles. Although it is not totally understood, we tentatively believe that these small nanobuckles might be related to the second-order buckling process of the silver nanowires.

We studied the kinetics of the silver nanobuckles by monitoring the same silver nanowires for over 20 days with polarized optical reflection microscope. As shown in Figure 3, series of optical micrographs of the stressed silver nanowires demonstrated significant changes when the silver nanobuckles were initialized and grown. With the graph taken 2 h after the sample preparation, the reflection (scattering) intensities of the silver nanowires are normal at all three locations that are marked with arrows (see Figure 3). The aligned silver nanowires demonstrated polarization dependent reflectivity. Similar results were observed by Shen and co-workers in their experiments of confocal white light
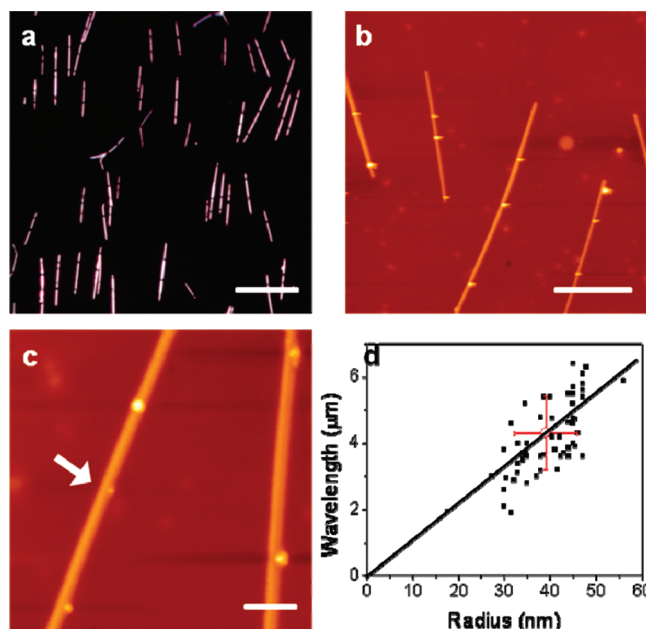

Figure 2. A graph of distance between silver nanobuckles with respect to silver nanowires diameter. (a) Optical reflection micrograph of silver nanobuckles along silver nanowires. Scale bar is 20 μm. (b) AFM image of nanobuckle on silver nanowire. Scale bar is 5 μm. (c) A higher resolution AFM image of silver nanobuckles. Scale bar is 1 μm. (d) The dependence of distance between silver nanobuckles with the diameter of silver nanowires.

reflection imaging of silver nanowires.[36] On the second day, we observed that a dark dot appears at the yellow arrow position on the graph with a (0,0) configuration, where we set white light source at a 0 degree and used a polarization filter at 0 degree before the camera. The 0-degree polarization is parallel to the vertical direction in the micrographs. As we discussed before, the dark dot along the silver nanowire indicates the existence of the nanobuckle at that position. However, such a dark dot cannot be observed in the micrograph obtained with a (90, 90) configuration. Similar polarization dependent phenomena were also observed by Halas and co-workers when they studied nanoparticle-mediated coupling of light into a silver nanowire, which originated from the confined plasmon propagating in one-dimensional silver nanowires.[17] On the other hand, excitation of longitudinal and transversal plasmon resonances in silver nanowires wrapped with gold nanoparticles was demonstrated to be critical in polarization dependence of Raman scattering from such nanoparticle−nanowire nanostructures.[37]

The polarization dependence on scattering at the nanobuckles is changing during the growth of the nanobuckles. In the (90, 90) configuration, the dark dot does show up at the yellow arrow position on the micrograph acquired at 96 h. Moreover, the size of the dark dot appears larger in the image (96 h) with (0,0) configuration than the one in the previous image (30 h). The larger dark dot is due to the larger size of nanobuckle, which is still growing during the 96 h. With these results, we conclude that the small
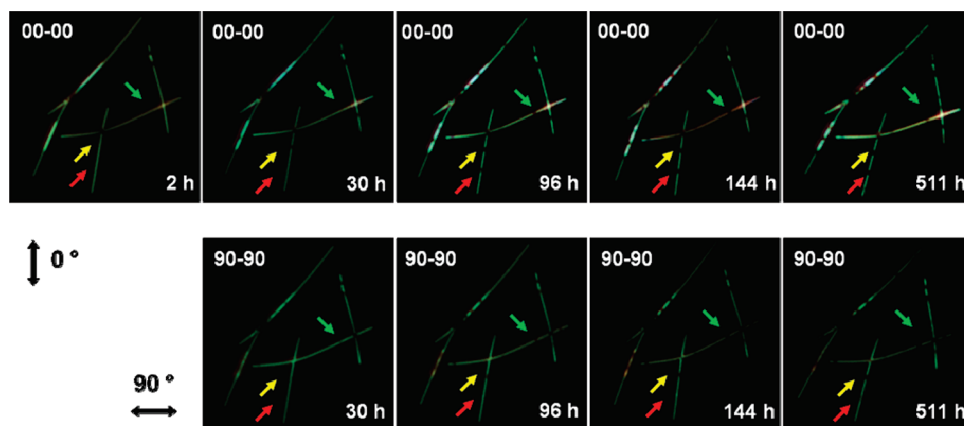
Figure 3. Optical reflection micrographs of the same silver nanowires captured at the different times. The images in the top row are captured at (0,0) configuration in polarization. The bottom row images are captured with a (90,90) configuration. Images are 25 × 25 μm².

nanobuckles are polarization-sensitive during their initial growth and such polarization sensitivity decreases with increasing nanobuckles size. For the silver nanobuckle shown with the red arrow, similar phenomena were observed. Its optical response can be observed in (0,0) micrographs started at 96 h, but there is no optical effect in micrograph (90,90) at 96 h. However, it appears as a brighter spot at 144 h, while finally converted to the usual dark dot at 511 h. Similar results were observed with the nanobuckle shown with the green mark, which first appears in (90,90) micrographs and then shows up in (0,0) images. The polarization measurements with (0,90) and (90,0) configurations were also conducted on the silver nanobuckles. As shown in the Supporting Information, the intensity is quite low due to the configuration of cross-polarization.

It is worth noting that in both cases of (0,90) and (90,0) configurations, the intensities of the nanobuckles are higher than the other parts of the silver nanowires. On the basis of the above observations, the dependence of the polarization during the nanobuckle growth could be related to their crystallinity or anisotropy.

The silver nanobuckles demonstrated interesting optical properties, such as photoplasmon conversion and emission from subwavelength structures. With the recent advances in plasmonic materials, integration of optics with nanomaterial has shown a great potential in future nano-opto devices.[38] Silver nanowires with well-developed crystal structures can be applied as surface plasmon resonators with a propagation length over 10 μm.[39,40] It was reported that the launch of propagating plasmon and subsequent emission of photons occur
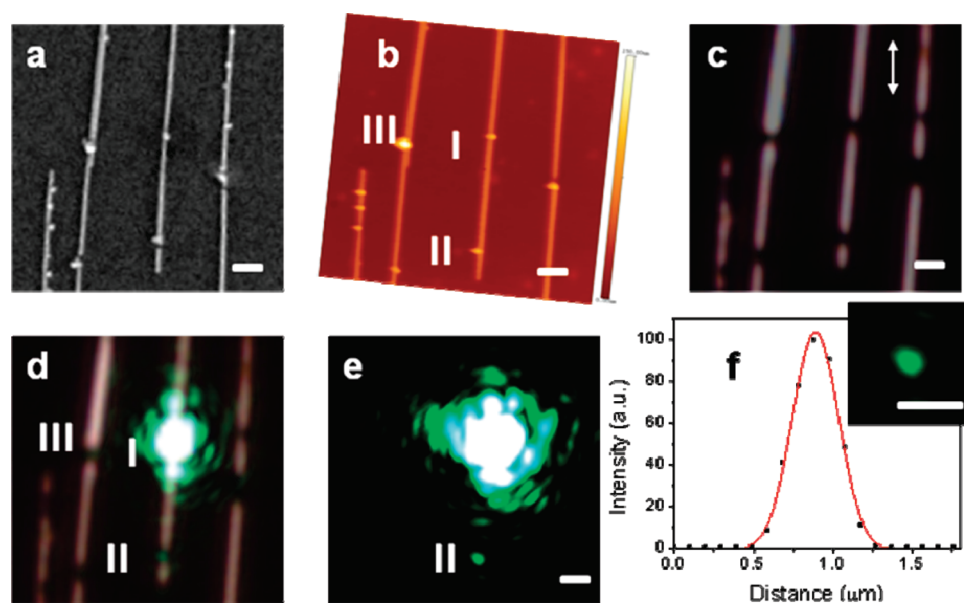

Figure 4. Propagating and scattering of plasmon with the nanobuckles on a silver nanowire: (a) SEM; (b) AFM, Z scale, 250 nm; (c) optical image of the same silver nanowire; (d) reflection graph of the silver nanowire when a green light is focused onto one nanobuckle; a green emission can be observed from its neighboring nanobuckle; (e) a clear image showing the scattered photon from the nanobuckle when the white-light source is turned off; (f) an intensity profile of emitting light from the nanobuckle. (Inset) A zoom-in micrograph of the emitting location. The scale bars in all images are 1 μm.

only at its ends and other discontinuities of the silver nanowires. Our silver nanobuckles can be acting as discontinuities and have an ability to emit photons.

Nanobuckles on the silver nanowire, as shown in Figure 4, were studied with various microscopic methods to explore their optical properties. As measured from the AFM image, the heights of silver nanobuckles are 152, 160, and 245 nm for locations I, II, and III, respectively (Figure 4b). It is clear that the sizes of the silver nanobuckles are much larger than the diameter of the nanowires. With the correct polarization of the incident light (shown as double-direction arrow in Figure 4c), the vertically oriented silver nanowires can be clearly observed in the optical reflection image. The brighter silver nanowires with respect to their underlying PDMS substrate are due to the stronger scattering of incident photons from silver nanowires than that of PDMS. The weak or dark spots along silver nanowires in the optical images are strongly correlated to the nanobuckles observed in SEM and AFM images of the same specimen. This is a direct proof that the silver nanobuckles can affect the photon scattering of the silver nanowires.

Furthermore, an emission of the photons can be observed from the silver nanobuckles when a plasmon is propagated along the silver nanowires. Figure 4d shows that when a green laser (532 nm) is focused to a diffraction-limit spot in one nanobuckle (location I), an emission of green light from its neighboring nanobuckle (location II) is observed. By turning off the white light, we can present a clearer image of the photon emission (Figure 4e). It is worth noting that the nanobuckle (location III) on another silver NW does *not* emit photons even though its distance to nanobuckle I (laser focus position) is shorter than that of nanobuckle II. These results confirm that light scattering from the focus position (nanobuckle I) would not result in the scattering at location II. As discussed by Sanders and coworker, plasmon can be launched by illuminating at one end of a silver nanowire or a sharp discontinuity along the nanowire surface, where the momentum of the incoming photon can be matched to that of the propagating plasmon.[41,42] The silver nanobuckles in our experiments can break the cylindrical symmetry of silver nanowires, which makes it possible to convert light into propagating axial plasmon modes. Therefore, we can conclude that the green light emitted from the nanobuckle at location II is a result of plasmon propagation incident upon a sharp discontinuity (the nanobuckle on the silver nanowire).

The profile analysis of the emitting spot reveals a perfect Gaussian fit for its intensity profile with a fwhm
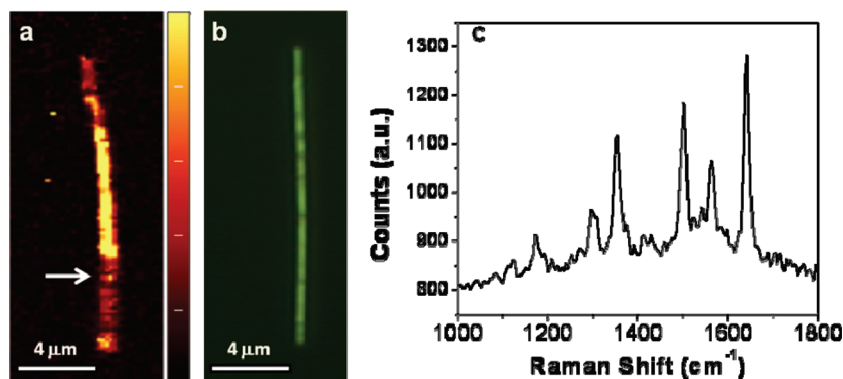

Figure 5. SERS of R6G adsorbed on the nanobuckles along silver nanowires: (a) confocal Raman mapping based on intensity of the R6G Raman peak at 1650 cm^{-1}, (b) optical image of the same silver nanowires with buckles. (c) Raman spectrum of R6G corresponding to the location indicated by an arrow mark in the Raman mapping.

of 343 nm (Figure 4f). Considering the optical parameter of the objective (NA 0.75), we can deduce that the small spot in the optical image is due to the diffraction limit of the 532 nm light that is emitted from the silver nanobuckle. It is obvious that the light source is much smaller than the wavelength of the emitted green light. As the results, the presence of nanobuckles along a silver nanowire can function as a subwavelength optical source in application such as optical waveguides. As shown in the inset of Figure 4f, the light emitted from silver nanobuckle has a perfect isotropic distribution.

The localized SERS was observed along the silver nanowires, as demonstrated for R6G Raman spectra collected with the confocal Raman microscopy. We performed confocal Raman mapping on five independent buckled silver nanowires. SERS enhancements were observed from all these buckled silver nanowires. Figure 5a shows a typical intensity map of Raman peak at 1650 cm^{-1} from the R6G molecules. It is obvious that SERS can be enhanced along the buckled silver nanowire. The dark area along the silver nanowire in the optical image of the same individual silver nanowire (Figure 5b) clearly indicates the presence of nanobuckles. Furthermore, we can correlate the regions of improved Raman enhancement with the presence of nanobuckles (see arrow in Figure 5a and spectrum in Figure 5c). It is also worth noting that high SERS activities are not always observed at all these silver nanobuckles, which can be related to the size of nanobuckles and the hot-spots that were created consequently. Experiments with SERS tests, AFM characterizations, and polarization measurements can further clarify the origin of the SERS enhancement. Such experiments are currently in progress and their detailed analysis will be published in near future. Our experimental results indicate that the presence of nanobuckles can improve the localized SERS enhancement. The effect on SERS enhancement could be due to the change of surface plasmon resonance in the vicinities of the nanobuckles.

It is a novel approach in fabricating nanoparticles on silver nanowires by using shear force to compress silver nanowires and further growing nanobuckles along the nanowires. In general, a variety of methods has been reported in the synthesis of nanoparticle/nanowire hybrids, such as using catalyst during the nanowire growth,[43] surface modification of nanorods,[44] *in situ* growth of nanoparticles on nanowires,[45,46] and self-assembly of nanoparticles along nanowires.[17,19] To the best of our knowledge, this is the first time that we demonstrated the possibility of growing nanoparticles alone buckled nanowires by using the compression stress. Unlike other approaches, the nanobuckles generated with this compression stress method have irregular shapes rather than smooth spherical particles, which could have interesting surface functionalities and unique applications in chemical catalysis and SERS-based chemical detections with anisotropic nanostructures.[47] For example, SERS enhancement at the junctions of silver nanowires was recently reported.[48] Further studies on the surface properties of the nanobuckles are in progress and the results will be reported elsewhere.

The detailed studies on mechanical buckling of silver nanowires discussed here provide useful information regarding the nanomechanical behavior of one-dimensional nanostructures. We clearly observed the growth of silver nanobuckles on particular nanowires with their optical properties for over 500 h. Furthermore, the slow process of the nanobuckle growth allows a detailed mechanism study, which is important in evaluating the mechanical stability of nanoscale materials and can be applied to the studies of the mechanical properties of other nanomaterials.

Our approach yields nanobuckles on silver nanowires with unique nanoscale structures that allow the coupling of light into the 1D plasmonic waveguides. Controlling the interaction of light and nanoscale optical material is critical for developing optical interconnects for on-chip integration.[49] It is a big challenge to couple light into, and out of, plasmon waveguide efficiently while compensating the momentum difference between photons and plasmons.[50] Recently, hybridization of adjacent nanostructures was reported and it was found that hybridized nanostructures could yield new plasmonic states.[51] Our experimental results indicated that the silver nanobuckles produced by means of mechanical compression could be utilized in the optical coupling process. Scattering lights with the diameter around 343 nm were obtained from the silver nanobuckles. Such subwavelength optical sources are due to the silver nanobuckles that can interfere with the propagation of the surface plasmon. With additional optimization, the nanobuckles on silver nanowire could have great potentials in nano-waveguide application, catalyst for chemical reactions, and nanostructured SERS templates. Uji-i and co-workers recently reported interesting research on the remote excitation of SERS on assembled nanowire/nanoparticle aggregate systems and obtained SERS spectra with much less background.[52] In our scenario, by using mechanical stimulation, we are able to manipulate the formation of the silver nanobuckles so that the nanoparticle/nanowire system could be precisely controlled. Consequently, such a complex nanostructure system might have great potentials in high-resolution SERS imaging devices.

EXPERIMENTAL DETAILS

Silver NWs were synthesized and purified according to a well-known procedure by using $AgNO_3$ precursor and poly(vinylpyrrolidone) (PVP) as a capping agent (Mn = 1.3×10^6 Da) as reported before.[53,54] PDMS elastomers were prepared by casting prepolymer Sylgard 185 and its kit with a ratio of 10:1 in a glass Petri dish. After a careful degassing for 30 min and curing at 70 °C for 2 h, the PDMS substrate is formed and ready for further sample preparation. The nanobuckles on silver NWs are formed by depositing the silver nanowires onto a prestrained PDMS substrate (Figure 1a−c). Methanol suspension of silver NWs were cast onto the surface of prestretched PDMS substrate and dried by using a N_2 gas flow. It is worth noting that the direction of drying is critical as to align the silver nanowires parallel to the direction in which the PDMS substrate is prestretched. The samples were allowed to dry overnight before the prestrained PDMS substrate was released. Because of the compressive-stress that is parallel to the direction of the silver NWs, nanoscale buckles were formed along the NWs within 3 days. We also observed the formation of nanobuckles even when the silver nanowires are not perfectly parallel to the prestretched direction of PDMS substrate (see an example in Figure 2a). However, according to the buckling theory, we would assume that the presence of these nanobuckles might need higher compression forces due to their nonparallel orientations.

The morphology and optical properties of silver nanobuckles were studied by optical microscope (polarized microscope and confocal microscope), AFM, and SEM. Optical microscopic investigation was conducted on an Aramis confocal microscope (Horiba Jobin Yvon, Edison, NJ) and an Ar ion laser (532 nm) was applied in the plasmonic propagation experiments. The optical micrographs were obtained by using 50× objective (NA = 0.75) and recorded with a three-megapixel CCD camera. Morphology and size of the silver nanobuckles were measured on a Nano-R_2 atomic force microscope (Pacific Nanotechnology Inc. Santa Clara, CA) with a tapping mode under ambient condition. Field-emission SEM (FE-SEM) micrographs of the silver nanobuckles were obtained on a scanning electron microscope, Jeol 6500, equipped with thermally assisted field emission gun. Before the FE-SEM imaging, a thin layer of Pt film was deposited on the sample so that the charging effect (cause by the nonconductive PDMS) can be significantly eliminated. A low accelerating voltage (5 kV) was used during the SEM imaging.

A R6G solution with concentration of 10^{-6} mol/L was used to evaluate the SERS of the nanobuckles on silver nanowires. The SERS experiments were conducted on either the Aramis microscope or an Alpha300R WiTec confocal Raman microscope (514 nm).[55] In the experiments with Aramis instrument, laser line (532 nm, ∼0.2 mW) was focused onto the sample with the spot size at a submicroregion. The sample was roster scanned, and the intensities of Raman peak at 1650 cm^{-1} were utilized to form

Raman maps. Integration time was 1 s. We further compared the Raman maps with normal optical images, and the correlation between the SERS enhancement and the structures of buckled silver nanowires were explored.

Supporting Information Available: Optical micrographs of the same buckled silver nanowires with various polarization configurations of white light source and camera. This material is available free of charge *via* the Internet at http://pubs.acs.org.

REFERENCES AND NOTES

1. Orendorff, C. J.; Gearheart, L.; Jana, N. R.; Murphy, C. J. Aspect Ratio Dependence on Surface Enhanced Raman Scattering Using Silver and Gold Nanorod Substrates. *Phys. Chem. Chem. Phys.* **2006**, *8*, 165–170.
2. Murphy, C. J.; Sau, T. K.; Gole, A. M.; Orendorff, C. J.; Gao, J. X.; Gou, L. F.; Hunyadi, S. E.; Li, T. Anisotropic Metal Nanoparticles: Synthesis, Assembly, and Optical Applications. *J. Phys. Chem. B* **2005**, *109*, 13857–13870.
3. Murphy, C. J.; Gole, A. M.; Hunyadi, S. E.; Stone, J. W.; Sisco, P. N.; Alkilany, A.; Kinard, B. E.; Hankins, P. Chemical Sensing and Imaging With Metallic Nanorods. *Chem. Commun.* **2008**, 544–557.
4. Khanal, B. P.; Zubarev, E. R. Purification of High Aspect Ratio Gold Nanorods: Complete Removal of Platelets. *J. Am. Chem. Soc.* **2008**, *130*, 12634–12635.
5. Kong, J.; Ferhan, A. R.; Chen, X.; Zhang, L.; Balasubramanian, N. Polysaccharide Templated Silver Nanowire for Ultrasensitive Electrical Detection of Nucleic Acids. *Anal. Chem.* **2008**, *80*, 7213–7217.
6. Zong, R.-L.; Zhou, J.; Li, Q.; Du, B.; Li, B.; Fu, M.; Qi, X.-W.; Li, L.-T.; Buddhudu, S. Synthesis and Optical Properties of Silver Nanowire Arrays Embedded in Anodic Alumina Membrane. *J. Phys. Chem. B* **2004**, *108*, 16713–16716.
7. Jana, N. R.; Gearheart, L.; Murphy, C. J. Wet Chemical Synthesis of Silver Nanorods and Nanowires of Controllable Aspect Ratio. *Chem. Commun.* **2001**, 617–618.
8. Guo, L. F.; Chipara, M.; Zaleski, J. M. Convenient, Rapid Synthesis of Ag Nanowires. *Chem. Mater.* **2007**, *19*, 1755–1760.
9. Zhu, Y. J.; Hu, X. L. Microwave-Assisted Polythiol Reduction Method: A New Solid−Liquid Route to Fast Preparation of Silver Nanowires. *Mater. Lett.* **2004**, *58*, 1517–1519.
10. Kundu, S.; Wang, K.; Liang, H. Size-Controlled Synthesis and Self-Assembly of Silver Nanoparticles within a Minute Using Microwave Irradiation. *J. Phys. Chem. C* **2009**, *113*, 134–141.
11. Braun, E.; Eichen, Y.; Sivan, U.; Ben-Yoseph, G. DNA-Templated Assembly and Electrode Attachment of a Conducting Silver Wire. *Nature* **1998**, *391*, 775–778.
12. Sloan, J.; Wright, D. M.; Woo, H. G.; Bailey, S.; Brown, G.; York, A. P. E.; Coleman, K. S.; Hutchison, J. L.; Green, M. L. H. Capillarity and Silver Nanowire Formation Observed in Single Walled Carbon Nanotubes. *Chem. Commun.* **1999**, 699–700.
13. Chimentäo, R. J.; Kirm, I.; Medina, F.; Rodriguez, X.; Cesteros, Y.; Salagre, P.; Sueiras, J. E. Different Morphologies of Silver Nanoparticles as Catalysts for the Selective Oxidation of Styrene in the Gas Phase. *Chem. Commun.* **2004**, 846–847.
14. Manjavacas, A.; de Abajo, F. J. G. Robust Plasmon Waveguides in Strongly Interacting Nanowire Arrays. *Nano Lett.* **2009**, *9*, 1285–1289.
15. Aroca, R. F.; Goulet, P. J. G.; Dos Santos, D. S.; Alvarez-Puebla, R. A.; Oliveira, O. N. Silver Nanowire Layer-by-Layer Films as Substrates for Surface-Enhanced Raman Scattering. *Anal. Chem.* **2005**, *77*, 378–382.
16. Akimov, A. V.; Mukherjee, A.; Yu, C. L.; Chang, D. E.; Zibrov, A. S.; Hemmer, P. R.; Park, H.; Lukin, M. D. Generation of Single Optical Plasmons in Metallic Nanowires Coupled to Quantum Dots. *Nature* **2007**, *450*, 402–406.
17. Knight, M. W.; Grady, N. K.; Bardhan, R.; Hao, F.; Nordlander, P.; Halas, N. J. Nanoparticle-Mediated Coupling of Light into a Nanowire. *Nano Lett.* **2007**, *7*, 2346–2350.
18. Fedutik, Y.; Temnov, V. V.; Schöps, O.; Woggon, U.; Artemyev, M. V. Exciton-Plasmon-Photon Conversion in Plasmonic Nanostructures. *Phys. Rev. Lett.* **2007**, *99*, 136802.
19. Tran, M. L.; Centeno, S. P.; Hutchison, J. A.; Engelkamp, H.; Liang, D. D.; Tendeloo, G. V.; Sels, B. F.; Hofkens, J.; Uji-I, H. Control of Surface Plasmon Localization *via* Self-Assembly of Silver Nanoparticles along Silver Nanowires. *J. Am. Chem. Soc.* **2008**, *130*, 17240–17241.
20. Chen, X.; Li, S.; Xue, C.; Banholzer, M. J.; Schatz, G. C.; Mirkin, C. A. Plasmonic Focusing in Rod-Sheath Heteronanostructures. *ACS Nano* **2009**, *3*, 87–92.
21. Qin, L.; Zou, S.; Xue, C.; Atkinson, A.; Schatz, G. C.; Mirkin, C. A. Designing, Fabrication, and Imaging Raman Hot Spots. *Proc. Natl. Acad. Sci. U.S.A.* **2006**, *103*, 1300–13303.
22. Qin, L.; Banholzer, M. J.; Millstone, J. E.; Mirkin, C. A. Nanodisk Codes. *Nano Lett.* **2007**, *7*, 3849–3853.
23. Wu, B.; Heidelberg, A.; Boland, J. J. Mechanical Properties of Ultrahigh-Strength Gold Nanowires. *Nat. Mater.* **2004**, *4*, 525–529.
24. Riaz, M.; Fulati, A.; Zhao, Q. X.; Nur, O.; Willander, M.; Klason, P. Buckling and Mechanical Instability of ZnO Nanorods Grown on Different Substrates under Uniaxial Compression. *Nanotechnology* **2008**, *19*, 415708.
25. Postma, H. W. Ch.; Teepen, T.; Yao, Z.; Grifoni, M.; Dekker, C. *Science* **2001**, *293*, 76–79.
26. Wang, Z. L.; Song, J. H. Piezoelectric Nanogenerators Based on Zinc Oxide Nanowire Arrays. *Science* **2006**, *312*, 242–246.
27. Leach, A. M.; McDowell, M.; Gall, K. Deformation of Top-Down and Bottom-Up Silver Nanowires. *Adv. Funct. Mater.* **2006**, *17*, 43–53.
28. Lucas, M.; Leach, A. M.; McDowell, M. T.; Hunyadi, S. E.; Gall, K.; Murphy, C. J.; Riedo, E. Plastic Deformation of Pentagonal Silver Nanowires: Comparison Between AFM Nanoindentation and Atomistic Simulations. *Phys. Rev. B* **2008**, *77*, 245420.
29. Li, X. D.; Gao, H. S.; Murphy, C. J.; Caswell, K. K. Nanoindentation of Silver Nanowires. *Nano Lett.* **2003**, *3*, 1495–1498.
30. Jing, G. Y.; Duan, H. L.; Sun, X. M.; Zhang, Z. S.; Xu, J.; Li, Y. D.; Wang, J. X.; Yu, D. P. Surface Effects on Elastic Properties of Silver Nanowires: Contact Atomic-Force Microscopy. *Phys. Rev. B* **2006**, *73*, 235409.
31. Chen, Y.; Dorgan, B. D., Jr; McIlroy, D. N.; Aston, D. E. On the Importance of Boundary Conditions on Nanomechanical Bending Behavior and Elastic Modulus Determination of Silver Nanowires. *J. Appl. Phys.* **2006**, *100*, 104301.
32. Gunawidjaja, R.; Ko, H.; Jiang, C.; Tsukruk, V. V. Buckling Behavior of Highly Oriented Silver Nanowires Encapsulated within Layer-by-Layer Films. *Chem. Mater.* **2007**, *19*, 2007–2015.
33. Khangm, D.-Y.; Xiao, J.; Kocabas, C.; MacLaren, S.; Banks, T.; Jiang, H.; Huang, Y. Y.; Rogers, J. A. Molecular Scale Buckling Mechanics in Individual Aligned Single-Wall Carbon Nanotubes on Elastomeric Substrates. *Nano Lett.* **2008**, *8*, 124–130.
34. Timoshenko, S. P. Goodier, J. N. *Theory of Elasticity*; McGraw-Hill: New York, 1970; Chapter 12.
35. Wu, B.; Heidelberg, A.; Boland, J. J.; Sader, J. E.; Sun, X.; Li, Y. Microstructure-Hardened Silver Nanowires. *Nano Lett.* **2006**, *6*, 468–472.

36. Du, C. L.; You, Y. M.; Kasim, J.; Ni, Z. H.; Yu, T.; Wong, C. P.; Fan, H. M.; Shen, Z. X. Confocal White Light Reflection Imaging for Characterization of Metal Nanostructures. *Opt. Commun.* **2008**, *281*, 5360–5363.

37. Gunawidjaja, R.; Peleshanko, S.; Ko, H.; Tsukruk, V. V. Bimetallic Nanocobs: Decorating Silver Nanowires with Gold Nanoparticles. *Adv. Mater.* **2008**, *20*, 1544–1549.

38. Sirbuly, D. J.; Law, M.; Yan, H.; Yang, P. Semiconductor Nanowires for Subwavelength Photonics Integration. *J. Phys. Chem. B* **2005**, *109*, 15190–15213.

39. Dickson, R. M.; Lyon, L. A. Unidirectional Plasmon Propagation in Metallic Nanowires. *J. Phys. Chem. B* **2000**, *104*, 6095–6098.

40. Ditlbacher, H.; Hohenau, A.; Wagner, D.; Kreibig, U.; Roger, M.; Hofer, F.; Aussenegg, F. R.; Krenn, J. R. Silver Nanowires as Surface Plasmon Resonators. *Phys. Rev. Lett.* **2005**, *95*, 257403.

41. Sanders, A. W.; Routenberg, D. A.; Wiley, B. J.; Xia, Y.; Dufresne, E. R.; Reed, M. A. Observation of Plasmon Propagation, Redirection, and Fan-Out in Silver Nanowires. *Nano Lett.* **2006**, *6*, 1822–1826.

42. Pyayt, A. L.; Wiley, B.; Xia, Y.; Chen, A.; Dalton, L. Integration of Photonic and Silver Nanowire Plasmonic Waveguides. *Nat. Nanotechnol.* **2008**, *3*, 660–665.

43. Jiang, C.; Zhao, J.; Therese, H. A.; Freidrich, M.; Mews, A. Raman Imaging and Spectroscopy of Heterogeneous Individual Carbon Nanotubes. *J. Phys. Chem. B* **2003**, *107*, 8742–8745.

44. Assmus, T.; Balasubramanian, K.; Burghard, M.; Kern, K.; Scolari, M.; Fu, N.; Myalistsin, A.; Mews, A. Raman Properties of Gold Nanoparticle-Decorated Individual Carbon Nanotubes. *Appl. Phys. Lett.* **2007**, *90*, 173109.

45. Fan, Y.; Burghard, M.; Kern, K. Chemical Defect Decoration of Carbon Nanotubes. *Adv. Mater.* **2002**, *14*, 130–133.

46. Pinto, R. J. B.; Marques, P. A. A. P.; Martins, M. A.; Neto, C. P.; Trindade, T. Electrostatic Assembly and Growth of Gold Nanoparticles in Cellulosic Fibres. *J. Colloid Interface Sci.* **2007**, *312*, 506–512.

47. Ko, H.; Singamaneni, S.; Tsukruk, V. V. Nanostructured Surfaces and Assemblies as SERS Media. *Small* **2008**, *4*, 1576–1599.

48. Gu, G. H.; Suh, J. S. Enhancement at the Junction of Silver Nanorods. *Langmuir* **2008**, *24*, 8934–8938.

49. Ozbay, E. Plasmonics: Merging Photonics and Electronics at Nanoscale Dimensions. *Science* **2006**, *311*, 189–193.

50. Law, M.; Sirbuly, D. J.; Johnson, J. C.; Goldberger, J.; Saybally, R. J.; Yang, P. Nanoribbon Waveguides for Subwavelength Photonics Integration. *Science* **2004**, *305*, 1269–1273.

51. Wang, H.; Brandl, D.; Nordlander, P.; Halas, N. J. Plasmonic Nanostructures: Artificial Molecules. *Acc. Chem. Res.* **2007**, *40*, 53–62.

52. Hutchison, J. A.; Centeno, S. P.; Odaka, H.; Fukumura, H.; Hofkens, J.; Uji-i, H. Subdiffraction Limited, Remote Excitation of Surface Enhanced Raman Scattering. *Nano Lett.* **2009**, *9*, 995–1001.

53. Gunawidjaja, R.; Jiang, C.; Peleshanko, S.; Ornatska, M.; Singamaneni, S.; Tsukruk, V. V. Flexible and Robust 2D Arrays of Silver Nanowires Encapsulated Within Freestanding Layer-by-Layer Films. *Adv. Funct. Mater.* **2006**, *16*, 2024–2034.

54. Tao, A.; Kim, F.; Hess, C.; Goldberger, J.; He, R.; Sun, Y; Xia, Y.; Yang, P. Langmuir−Blodgett Silver Nanowire Monolayers for Molecular Sensing Using Surface-Enhanced Raman Spectroscopy. *Nano Lett.* **2003**, *3*, 1229–1233.

55. Ko, H.; Chang, S.; Tsukruk, V. V. Porous Substrates for Label-Free Molecular Level Detection of Nonresonant Organic Molecules. *ACS Nano* **2009**, *3*, 181–188.